Polymer Chemistry

ROYAL SOCIETY OF CHEMISTRY

PAPER

View Article Online
View Journal | View Issue

Cite this: *Polym. Chem.*, 2023, **14**, 5060

Thermoresponsive property of poly(*N*,*N*-bis(2-ethoxyethyl)acrylamide) and its multiblock copolymers with poly(*N*,*N*-dimethylacrylamide) prepared by hydrosilylation-promoted group transfer polymerization†

Xiangming Fu, [a] Yanqiu Wang,[a] Liang Xu,[a] Atsushi Narumi, [b] Shin-ichiro Sato, [c] Xiaoran Yang,[a] Xiande Shen*[a,d] and Toyoji Kakuchi *[a,c,d]

Poly(*N*,*N*-bis(2-ethoxyethyl)acrylamide) (PEOEAm), a new thermoresponsive polyacrylamide, has been studied from the perspectives of synthesis and thermal phase transition. PEOEAm without any initiator residue at the chain end was synthesized *via* hydrosilylation-promoted group transfer polymerization (GTP) to exclude the effect of polymer end groups on the thermoresponsive properties of the polymer. To extend thermoresponsive PEOEAm to its copolymer systems, the GTP tendency of EOEAm was evaluated and compared with that of *N*,*N*-dimethylacrylamide (DMAm). There exists a significant difference between the polymerization reactivities of EOEAm and DMAm, and this difference was applied to realize the random group transfer copolymerization (GTcoP) of EOEAm ("A" unit) and DMAm ("B" unit) for the one-pot synthesis of a BA-block copolymer. A series of block copolymer architectures, such as AB-, ABA-, BAB-, and BABA-block copolymers, were similarly prepared. The thermoresponsive properties of the block copolymers were evaluated by measuring the cloud-point temperature and hydrodynamic radius of their aqueous solutions.

Received 10th September 2023,
Accepted 28th October 2023

DOI: 10.1039/d3py01032e

rsc.li/polymers

Introduction

Smart polymers can respond to various stimuli such as heat, light, pH, and magnetic and electric fields. Changes have been observed in individual properties such as hydrophilicity and hydrophobicity, sol–gel properties, and crystallinity, as well as in combinations of these properties, of these materials before and after they respond to such stimuli.[1–8] For example, aqueous solutions of certain polymers exhibit reversible phase transition behavior, turning turbid when heated to a temperature above the lower critical solution temperature (LCST) and turning back to a clear solution upon dissolution when cooled below the LCST.[9–14] One of the molecular design approaches adopted in the synthesis of thermoresponsive polymers is to balance the water solubility and hydrophobicity of the polymers.[15–17] Among representative thermoresponsive polymers such as poly(*N*-substituted (meth)acrylamide), polyethers, and cellulose derivatives, poly(*N*-isopropylacrylamide) (PNIPAM) has shown potential for chemical and biological applications in controlled drug delivery, bioconjugation, tissue engineering, and bioseparation, as well as in biosensors.[18–21] Therefore, the phase transition behavior of PNIPAM has been studied using analytical methods such as turbidimetric, calorimetric, nuclear magnetic resonance, fluorescence, light scattering, and neutron scattering analyses.[22–24] With regard to the synthetic chemistry of thermoresponsive poly(*N*-substituted (meth)acrylamide), there are two important challenges: the expansion of applicable monomers and the synthesis of well-defined polymers through precise polymerization. Many thermoresponsive poly(*N*-substituted acrylamides), including PNIPAM, are known, and various polymer architectures have

[a]*Research Center for Polymer Materials, School of Materials Science and Engineering, Changchun University of Science and Technology, Weixing Road 7989, Jilin 130022, China. E-mail: kakuchi@eng.hokudai.ac.jp; Fax: +81-11-706-6602; Tel: +81-11-706-6602*
[b]*Graduate School of Organic Materials Science, Yamagata University, 4-3-16 Jonan, Yonezawa, Yamagata 992-8510, Japan*
[c]*Division of Applied Chemistry, Faculty of Engineering, Faculty of Engineering, Hokkaido University, Sapporo, Hokkaido 060-8628, Japan*
[d]*Chongqing Research Institute, Changchun University of Science and Technology, No. 618 Liangjiang Avenue, Longxing Town, Yubei District, Chongqing City 401135, China*

† Electronic supplementary information (ESI) available. See DOI: https://doi.org/10.1039/d3py01032e

been designed, synthesized, and used in a variety of applications. In contrast, poly(*N*,*N*-disubstituted acrylamide) (PDSAm) has two different combinations of *N*,*N*-disubstituents: (1) one type comprises PDSAm with two different *N*-substituents to balance water solubility and hydrophobicity, and these *N*,*N*-disubstituents can cause thermal responses. Examples of this type are *N*-ethyl,*N*-methyl, *N*-methyl,*N*-*n*-propyl, *N*-methyl,*N*-isopropyl, *N*-ethyl,*N*-(2-methoxylethyl), *N*-(2-methoxylethyl),*N*-*n*-propyl, and *N*-(2-methoxylethyl),*N*-isopropyl groups.[25–30] (2) The other type comprises thermoresponsive PDSAm with two identical *N*-substituents and is limited to poly(*N*,*N*-diethylacrylamide) (PDEAm), poly(*N*,*N*-bis(2-methoxyethyl)acrylamide) (PMOEAm), poly(*N*-acryloylpyrrolidine), and poly(*N*-acryloylpiperidine) because of the limited number of suitable *N*-substituents compared to the first type.[31–34] Although PDEAm and PMOEAm have been used predominantly, it will be very interesting to explore the PDSAm family to determine how the balance between water solubility and hydrophobicity affects thermoresponsive polymers.

Precise synthesis of PDSAm and its derivatives has been realized using controlled/living radical and anionic polymerizations of *N*,*N*-disubstituted acrylamide (DSAm).[35–38] We developed the hydrosilylation-promoted group transfer polymerization (GTP) of DSAm with hydrosilane ($HSiR_3$) using tris(pentafluorophenyl) borane ($B(C_6F_5)_3$) as a catalyst. This method is a certain and reliable method for producing PDSAm with both ends capped with hydrogen due to initiation and termination reactions. This method can provide important insights into the intrinsic thermoresponsive properties of PDSAm, unaffected by its chain-end groups.[39–42] In this paper, we reported the synthesis of poly(*N*,*N*-bis(2-ethoxyethyl) acrylamide) (PEOEAm) by the hydrosilylation-promoted GTP of *N*,*N*-bis(2-ethoxyethyl)acrylamide (EOEAm) using Me_2EtSiH and $B(C_6F_5)_3$, as shown in Scheme 1. The polymerization reactivity of EOEAm was revealed by comparing the polymerization kinetics and monomer reactivity ratios of EOEAm and *N*,*N*-dimethylacrylamide (DMAm). The hydrosilylation-promoted group transfer copolymerization (GTcoP) of EOEAm and DMAm was applied to prepare di-, tri-, and tetra-block copolymers. The thermoresponsive behaviors of PEOEAm and its block copolymers were discussed by measuring the cloud-point temperature (T_{cp}) and the aggregation properties below and above the T_{cp}.

Experimental

Measurements

^{1}H nuclear magnetic resonance (NMR) spectra were recorded by using a Bruker Avance III HD 500. Polymerization solutions were prepared in a Mikrouna glove box equipped with a gas purification system (molecular sieves and a copper catalyst) under a dry Ar atmosphere (H_2O and O_2 contents <1 ppm). The moisture and oxygen contents in the glove box were monitored by using MK-XTR-100 and MK-OX-SEN-1 sensors, respectively. The number-average molecular mass ($M_{n,SEC}$) and molecular mass distribution ($Đ$) of the polymers were measured by size-exclusion chromatography (SEC) at 40 °C using an Agilent high-performance liquid chromatography system (1260 Infinity II) in *N*,*N*-dimethylformamide (DMF) containing lithium chloride (0.01 mol L^{-1}) at a flow rate of 1.0 mL min^{-1} using Agilent Polar Gel–M (exclusion limit, 2×10^4 g mol^{-1}) and Polar Gel–M (exclusion limit, 4×10^6 g mol^{-1}) columns (7.5 × 300 mm; average bead size, 5 μm). Cloud-point measurements were performed using an ultraviolet–visible (UV–vis) spectrophotometer (Jasco V-770, Tokyo, Japan) equipped with a Jasco CTU-100 temperature controller. The path length was 10 mm, and temperature increased at a rate of 1 °C min^{-1}. Changes in transmittance with increasing temperature were recorded at a wavelength of 500 nm. The hydrodynamic radii (R_h) of the obtained polymers were analyzed using a Dyna Pro Nanostar® (Wyatt Technology, Santa Barbara, CA, USA) with a heating rate of 10 °C min^{-1}.

Materials

Dichloromethane (CH_2Cl_2, >99.5%; water content, <0.001%), methanol (MeOH), and calcium hydride (CaH_2) were purchased from Kanto Chemicals Co., Inc. Bis(2-ethoxyethyl) amine, *N*,*N*-dimethylacrylamide (DMAm), and dimethylethylsilane (Me_2EtSiH) were purchased from Tokyo Kasei Kogyo Co., Ltd. Tris(pentafluorophenyl)borane ($B(C_6F_5)_3$) was purchased from Wako Pure Chemical Industries, Ltd, and used after recrystallization from *n*-hexane at −30 °C. DMAm was distilled from CaH_2, degassed in three freeze–pump–thaw cycles, and stored under an Ar atmosphere prior to use. All other chemicals were purchased from available suppliers and used without purification. All polymerizations were performed in a glove box under an Ar atmosphere at 25 °C.

Synthesis of EOEAm

A solution of acryloyl chloride (22.6 mL, 25.2 g, 0.278 mol) in CH_2Cl_2 (80 mL) was added with stirring to a solution of bis(2-ethoxyethyl)amine (46.1 mL, 41.0 g, 0.254 mol) and triethylamine (53.0 mL, 38.6 g, 0.382 mol) in CH_2Cl_2 (700 mL) at 0 °C. The reaction mixture was allowed to warm up to ambient

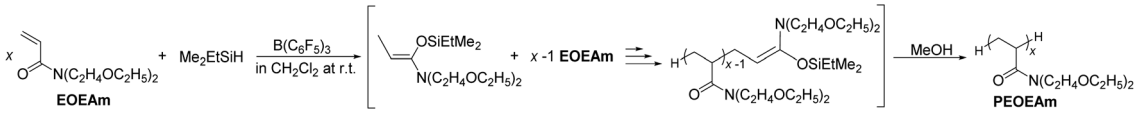

Scheme 1 Synthetic pathway of poly(*N*,*N*-bis(2-ethoxyethyl)acrylamide) (PEOEAm) by the hydrosilylation-promoted group transfer polymerization (GTP) of *N*,*N*-bis(2-ethoxyethyl)acrylamide (EOEAm).

temperature and was stirred overnight. The precipitated triethylammonium hydrochloride was filtered and washed with CH_2Cl_2 (2 × 100 mL). Subsequently, the combined organic solutions were extracted with 1 M HCl (3 × 100 mL), water (100 mL), and brine (200 mL). The organic layer was dried over anhydrous $MgSO_4$, and the solvent was removed under reduced pressure. The raw product was purified by vacuum distillation (154 °C/945 mbar) to obtain a viscous liquid. Yield, 32.9 g (60%). Anal. Calcd for $C_{12}H_{22}O_2Si$ (226.39): C, 61.37; H, 9.83; N, 6.51. Found: C, 61.41; H, 9.81; N, 6.49. ^{1}H NMR (500 MHz in $CDCl_3$, δ in ppm): 1.18 (t, 6H, –CH_3), 3.47 (q, 4H, –O–C$\underline{H}_2$CH$_3$), 3.55 (t, 2H, –NC$\underline{H}_2$–), 3.62 (dd, 4H, –O–C$\underline{H}_2$C$\underline{H}_2$N–), 3.64 (t, 2H, –NC$\underline{H}_2$–), 5.66 (dd, 1H, C$\underline{H}^E$=CH–CO), 6.32 (dd, 1H, C$\underline{H}^Z$=CH–CO), 6.68 (dd, 1H, =C$\underline{H}$–C=O). ^{13}C NMR (125 MHz in $CDCl_3$, δ in ppm): 15.10 (–CH_3), 47.32 and 49.09 (–NCH_2–), 66.40 and 66.78 (–O$\underline{C}H_2CH_3$), 68.75 and 68.86 (–NCH$_2\underline{C}$H$_2$–), 127.24 ($\underline{C}H_2$=CH–), 128.14 (=$\underline{C}$H–CO–), 166.88 (–CO).

Synthesis of PEOEAm

A typical polymerization procedure was conducted as follows (Procedure A): a solution of EOEAm (861.2 mg, 4.0 mmol), Me_2EtSiH (5.28 × 10^{-3} mL, 0.04 × 10^{-3} mmol), and $B(C_6F_5)_3$ (2.1 mg, 0.004 × 10^{-3} mmol) in CH_2Cl_2 (3.96 mL) was stirred for 12 h at 25 °C in a glove box under an Ar atmosphere. A small amount of methanol was added to terminate the polymerization. Subsequently, the crude product was purified by dialysis against acetone to obtain a primrose yellow solid product. Yield, 432.8 mg (50%); M_n, 21.8 kg mol^{-1}; M_w/M_n, 1.11 (run 4, Table 1).

Synthesis of PDMAm-*b*-PEOEAm

A typical random copolymerization was conducted as follows: Procedure A was performed using Me_2EtSiH (5.28 × 10^{-3} mL, 0.04 × 10^{-3} mmol), EOEAm (430.6 mg, 2.0 mmol), DMAm (198.4 mg, 2.0 mmol), $B(C_6F_5)_3$ (10.4 mg, 0.02 × 10^{-3} mmol), and CH_2Cl_2 (3.96 mL). The polymerization was conducted for 24 h and then terminated by adding methanol to obtain PDMAm-*b*-PEOEAm as a solid polymer. Yield, 413.5 mg (58%); M_n, 15.8 kg mol^{-1}; M_w/M_n, 1.09 (run 16, Table 2).

Synthesis of PEOEAm-*b*-PDMAm

A typical block copolymerization was conducted as follows: Procedure A was performed using Me_2EtSiH (5.28 × 10^{-3} mL, 0.04 × 10^{-3} mmol), EOEAm (430.6 mg, 2.0 mmol), $B(C_6F_5)_3$ (20.8 mg, 0.04 × 10^{-3} mmol), and CH_2Cl_2 (0.36 × 10^{-3} mL) for 12 h. An appropriate amount of the reaction solution was sampled to confirm the quantitative consumption of EOEAm by ^{1}H NMR measurements, and then a solution of DMAm (198.4 mg, 2.0 mmol) in CH_2Cl_2 (3.6 mL) was added to the polymerization mixture, and then this mixture was stirred for 24 h. PEOEAm-*b*-PDMAm was obtained as a white solid polymer. Yield, 381.2 mg (53%); M_n, 15.4 kg mol^{-1}; M_w/M_n, 1.10 (run 9, Table 2).

Synthesis of PDMAm-*b*-PEOEAm-*b*-PDMAm

A typical random copolymerization was conducted as follows: Procedure A was performed using Me_2EtSiH (5.28 × 10^{-3} mL, 0.04 × 10^{-3} mmol), EOEAm (430.6 mg, 2.0 mmol), DMAm (99.8 mg, 1.0 mmol), $B(C_6F_5)_3$ (20.8 mg, 0.04 × 10^{-3} mmol), and CH_2Cl_2 (2.3 mL) for 24 h. After confirming the quantitative consumption of EOEAm and DMAm by ^{1}H NMR measurements, a solution of DMAm (99.8 mg, 1.0 mmol) in CH_2Cl_2 (0.9 mL) was added to the polymerization mixture, and then the mixture was stirred for 12 h. PDMAm-*b*-PEOEAm-*b*-PDMAm was obtained as a white solid polymer. Yield, 411.1 mg (57%); M_n, 15.8 kg mol^{-1}; M_w/M_n, 1.12 (run 23, Table 3).

Synthesis of PEOEAm-*b*-PDMAm-*b*-PEOEAm

A typical random copolymerization was conducted as follows: Procedure A was performed using Me_2EtSiH (5.28 × 10^{-3} mL, 0.04 × 10^{-3} mmol), EOEAm (215.3 mg, 1.0 mmol), and $B(C_6F_5)_3$ (20.8 mg, 0.04 × 10^{-3} mmol) in CH_2Cl_2 (0.71 × 10^{-3} mL) for 6 h. After confirming the quantitative consumption of EOEAm by ^{1}H NMR measurements, a solution of DMAm (199.6 mg, 2.0 mmol) and EOEAm (215.3 mg, 1.0 mmol) in CH_2Cl_2 (2.58 mL) was added to the polymerization mixture, and then the mixture was stirred for 24 h. PEOEAm-*b*-PDMAm-*b*-PEOEAm was obtained as a white solid polymer. Yield, 395.9 mg (55%); M_n, 15.6 kg mol^{-1}; M_w/M_n, 1.12 (run 30, Table 3).

Table 1 Hydrosilylation-promoted group transfer polymerization (GTP) of EOEAm with Me_2EtSiH using $B(C_6F_5)_3$ as the catalyst [a]

Run	Polymer	$[EOEAm]_0/[Me_2EtSiH]_0/[B(C_6F_5)_3]_0$	Time/h	$M_{n,calcd}$[b]/kg mol^{-1}	$M_{n,MALS}$[c] (M_w/M_n[d])/kg mol^{-1}	T_{cp}[e]/°C
1	$PEOEAm_{25}$	25/1/0.1	6	5.4	5.4 (1.15)	14.5
2	$PEOEAm_{50}$	50/1/0.1	12	10.8	10.5 (1.15)	13.9
3	$PEOEAm_{75}$	75/1/0.1	12	16.1	15.9 (1.12)	8.9
4	$PEOEAm_{100}$	100/1/0.1	12	21.5	21.8 (1.11)	8.0
5	$PEOEAm_{150}$	150/1/0.5	24	32.3	31.8 (1.10)	5.9
6	$PEOEAm_{200}$	200/1/0.5	24	43.0	42.5 (1.10)	5.0

[a] $[EOEAm]_0$, 1.0 mol L^{-1}; solvent, CH_2Cl_2; temp., 25 °C; Ar atmosphere; monomer conversion determined by ^{1}H NMR in $CDCl_3$, >99.9%. [b] Calculated using the equation $[EOEAm]_0/[Me_2EtSiH]_0$ × (conv.) × (M.W. of the monomer) + (M.W. of H) × 2. [c] Determined by size-exclusion chromatography (SEC) using an instrument equipped with a multi-angle light scattering (MALS) detector in DMF containing lithium chloride (0.01 mol L^{-1}), dn/dc = 0.0344. [d] Determined by SEC using an instrument equipped with a refractive index (RI) detector in DMF containing lithium chloride (0.01 mol L^{-1}) using PMMA standards. [e] Determined by ultraviolet–visible light (UV–vis) measurements in water (10 g L^{-1}).

Table 2 Thermoresponsive properties of PEOEAm-*b*-PDMAm and PDMAm-*b*-PEOEAm by one-pot synthesis using the hydrosilylation-promoted group transfer copolymerization (GTcoP) of EOEAm (M_1) and DMAm (M_2) with Me_2EtSiH (SiH) using $B(C_6F_5)_3$ as the catalyst[a]

Run	Polymer	Block GTcoP: 1st GTP[b] $[M_1]_0/[SiH]_0$	Block GTcoP: 2nd GTP $[M_2]_0/[SiH]_0$	Random GTcoP[c] $[M_1]_0/[M_2]_0$	$M_{n,calcd}$/kg mol^{-1}	$M_{n,SEC}$ (M_w/M_n)[d]/kg mol^{-1}	T_{cp}[e]/°C
7	$PEOEAm_{30}$-*b*-$PDMAm_{70}$	30	70		13.4	13.3 (1.11)	33.0
8	$PEOEAm_{40}$-*b*-$PDMAm_{60}$	40	60		14.6	14.5 (1.09)	29.0
9	$PEOEAm_{50}$-*b*-$PDMAm_{50}$	50	50		15.7	15.4 (1.10)	25.0
10	$PEOEAm_{60}$-*b*-$PDMAm_{40}$	60	40		16.9	17.2(1.11)	23.1
11	$PEOEAm_{70}$-*b*-$PDMAm_{30}$	70	30		18.0	17.9 (1.09)	20.5
12	$PEOEAm_{80}$-*b*-$PDMAm_{20}$	80	20		19.2	19.3 (1.10)	20.0
13	$PEOEAm_{90}$-*b*-$PDMAm_{10}$	90	10		20.4	19.9 (1.12)	13.8
14	$PDMAm_{70}$-*b*-$PEOEAm_{30}$			30/70	13.4	13.4 (1.12)	33.6
15	$PDMAm_{60}$-*b*-$PEOEAm_{40}$			40/60	14.6	14.4 (1.11)	27.0
16	$PDMAm_{50}$-*b*-$PEOEAm_{50}$			50/50	15.7	15.8 (1.09)	25.1
17	$PDMAm_{40}$-*b*-$PEOEAm_{60}$			60/40	16.9	16.7 (1.11)	22.0
18	$PDMAm_{30}$-*b*-$PEOEAm_{70}$			70/30	18.0	18.4 (1.12)	21.5
19	$PDMAm_{20}$-*b*-$PEOEAm_{80}$			80/20	19.2	19.6 (1.10)	19.0
20	$PDMAm_{10}$-*b*-$PEOEAm_{90}$			90/10	20.4	20.1 (1.09)	14.0

[a] Solvent, CH_2Cl_2 temp., 25 °C; Ar atmosphere; monomer conversion determined by ^{1}H NMR spectra in $CDCl_3$, >99.9%. [b] $[EOEAm]_0$, 1.0 mol L^{-1}; $[SiH]_0/[B(C_6F_5)_3]_0$, 1.0; time, 12 h (1st GTP) and 24 h (2nd GTP). [c] $[M_1 + M_2]_0/[SiH]_0/[B(C_6F_5)_3]_0$, 100/1/0.5; time, 24 h. [d] Determined by an SEC instrument equipped with an RI detector in DMF containing lithium chloride (0.01 mol L^{-1}) using PMMA standards. [e] Determined by UV–vis measurements in water (10 g L^{-1}).

Table 3 Thermoresponsive properties of PDMAm-*b*-PEOEAm-*b*-PDMAm and PEOEAm-*b*-PDMAm-*b*-PEOEAm by one-pot synthesis using the hydrosilylation-promoted GTcoP of EOEAm (M_1) and DMAm (M_2) with Me_2EtSiH (SiH) using $B(C_6F_5)_3$ as the catalyst[a]

Run	Polymer	1st GTcoP[b] and 2nd GTP: $[M_1 + M_2]_0/[SiH]_0$	1st GTcoP[b] and 2nd GTP: $[M_2]_0/[SiH]_0$	1st GTP[c] and 2nd GTcoP: $[M_1]_0/[SiH]_0$	1st GTP[c] and 2nd GTcoP: $[M_1 + M_2]_0/[SiH]_0$	$M_{n,calcd}$/kg mol^{-1}	$M_{n,SEC}$ (M_w/M_n)[d]/kg mol^{-1}	T_{cp}[e]/°C
21	$PDMAm_{35}$-*b*-$PEOEAm_{30}$-*b*-$PDMAm_{35}$	(30 + 35)/1	35/1			13.4	13.5 (1.10)	—[f]
22	$PDMAm_{30}$-*b*-$PEOEAm_{40}$-*b*-$PDMAm_{30}$	(40 + 30)/1	30/1			14.6	14.6 (1.09)	—[f]
23	$PDMAm_{25}$-*b*-$PEOEAm_{50}$-*b*-$PDMAm_{25}$	(50 + 25)/1	25/1			15.7	15.8 (1.12)	—[f]
24	$PDMAm_{20}$-*b*-$PEOEAm_{60}$-*b*-$PDMAm_{20}$	(60 + 20)/1	20/1			16.9	17.1 (1.11)	34.8
25	$PDMAm_{15}$-*b*-$PEOEAm_{70}$-*b*-$PDMAm_{15}$	(70 + 15)/1	15/1			18.0	17.9 (1.10)	30.5
26	$PDMAm_{10}$-*b*-$PEOEAm_{80}$-*b*-$PDMAm_{10}$	(80 + 10)/1	10/1			19.2	19.3 (1.11)	24.2
27	$PDMAm_5$-*b*-$PEOEAm_{90}$-*b*-$PDMAm_5$	(90 + 5)/1	5/1			20.4	20.5 (1.12)	19.5
28	$PEOEAm_{15}$-*b*-$PDMAm_{70}$-*b*-$PEOEAm_{15}$			15/1	(15 + 70)/1	13.4	13.4 (1.11)	—[f]
29	$PEOEAm_{20}$-*b*-$PDMAm_{60}$-*b*-$PEOEAm_{20}$			20/1	(20 + 60)/1	14.6	14.5 (1.10)	39.6
30	$PEOEAm_{25}$-*b*-$PDMAm_{50}$-*b*-$PEOEAm_{25}$			25/1	(25 + 50)/1	15.7	15.6 (1.12)	34.9
31	$PEOEAm_{30}$-*b*-$PDMAm_{40}$-*b*-$PEOEAm_{30}$			30/1	(30 + 40)/1	16.9	17.0 (1.10)	30.8
32	$PEOEAm_{35}$-*b*-$PDMAm_{30}$-*b*-$PEOEAm_{35}$			35/1	(35 + 30)/1	18.0	18.1 (1.13)	26.9
33	$PEOEAm_{40}$-*b*-$PDMAm_{20}$-*b*-$PEOEAm_{40}$			40/1	(40 + 20)/1	19.2	19.5 (1.12)	21.0
34	$PEOEAm_{45}$-*b*-$PDMAm_{10}$-*b*-$PEOEAm_{45}$			45/1	(45 + 10)/1	20.4	20.4 (1.11)	16.7

[a] Solvent, CH_2Cl_2; $[SiH]_0/[B(C_6F_5)_3]_0$, 1.0; temp., 25 °C; Ar atmosphere; monomer conversion determined by ^{1}H NMR spectra in $CDCl_3$, >99.9%. [b] $[M_1 + M_2]_0$, 1.0 mol L^{-1}; time, 24 h (1st GTcoP), 12 h (2nd GTP, runs 21–24) and 6 h (2nd GTP, runs 25–27). [c] $[M_1]_0$, 1.0 mol L^{-1}; time, 6 h (1st GTP, runs 28–32), 12 h (1st GTP, runs 33 and 34), and 24 h (2nd GTP). [d] Determined by an SEC instrument equipped with an RI detector in DMF containing lithium chloride (0.01 mol L^{-1}) using PMMA standards. [e] Determined by UV–vis measurements in water (10 g L^{-1}). [f] Insoluble in water.

Results and discussion

Hydrosilylation-promoted GTP of EOEAm

EOEAm was prepared by the reaction of bis(2-ethoxyethyl) amine and acryloyl chloride. The ^{1}H and ^{13}C NMR spectra of EOEAm and its polymer are shown in Fig. S1.† Two signals at 47.32 and 49.09 ppm corresponding to the –N$\underline{C}H_2$– group, at 66.40 and 66.78 ppm corresponding to the –O$\underline{C}H_2CH_3$ group, and at 68.75 and 68.86 ppm corresponding to the –NCH$_2\underline{C}$H$_2$– group are observed in the ^{13}C NMR spectrum (Fig. S1c†); these signals are attributed to the *cis* and *trans* conformers of EOEAm. However, they exhibited identical polymerization reactivity, as confirmed by the fact that both were consumed equally as polymerization progressed. The conventional GTP method, in which the SKA initiator is used as one of the GTP components, yields polymers with SKA residues attached to

the α-terminus. In contrast, the hydrosilylation-promoted GTP method, in which SKA is generated by the 1,4-hydrosilylation of the monomer and hydrosilane in the polymerization system, yields polymers consisting only of repeating monomer units. Since the thermal properties of the thermoresponsive polymers in aqueous solutions are affected by the molecular mass and terminal substituents, the hydrosilylation-promoted GTP method was used to synthesize PEOEAm. We first described the result for the polymerization of EOEAm using Me_2EtSiH and $B(C_6F_5)_3$ in CH_2Cl_2 with a ratio $[EOEAm]_0/[Me_2EtSiH]_0/[B(C_6F_5)_3]_0$ = 25/1/0.5 at 25 °C. The obtained polymer exhibited a unimodal SEC with a relatively low molecular mass distribution ($Đ$) of 1.20, as shown in Fig. 1. The number-average molecular mass determined by multi-angle light scattering (MALS) ($M_{n,MALS}$) was 5.4 kg mol^{-1}; this result agrees with the calculated number-average molecular mass ($M_{n,calcd}$) of 5.4 kg mol^{-1}.

The ^{1}H (Fig. S1b†) and ^{13}C NMR spectra (Fig. S1d†) of the obtained polymer showed signals attributed to methylene and methine protons at 1.25–1.90 and 2.15–2.75 ppm, respectively, and those attributed to vinyl methylene and methine carbons at 45–50 and 34–38 ppm, respectively. A more detailed chemical structure of the obtained polymer is revealed in the results of matrix assisted laser desorption/ionization-time of flight mass spectrometry (MALDI-TOF MS). As shown in Fig. 2, only one series of molecular ion peaks was observed, and the distance between two adjacent molecular ion peaks was 215.3 Da, which agreed with the predicted molecular mass of 215.29 Da for EOEAm as the constitutional repeating unit. In addition, the m/z value of each molecular ion peak clearly indicated the sodium-cationized polymer composition of $[H\text{-}EOEAm_n\text{-}H + Na]^+$ (molecular formula: $C_{11n} + H_{21n} + N_n + O_{3n} + 2Na$); for instance, an m/z value of 5407.2 Da for a specified peak corresponds to a sodium-cationized 25-mer polymer structure of $[H\text{-}EOEAm_{25}\text{-}H + Na^+]$ with a theoretical monoisotopic value of 5407.33 for the molecular formula of $C_{275}H_{527}N_{25}O_{75}Na$. This result strongly supported our supposition that the hydrosilylation-promoted GTP of EOEAm was well controlled without any side reactions to produce the polymer with a planned degree of polymerization (DP) of 25, *i.e.*, $PEOEAm_{25}$. PEOEAm with a higher molecular mass was prepared by the $B(C_6F_5)_3$-catalyzed GTP of EOEAm and Me_2EtSiH with varying $[EOEAm]_0/[Me_2EtSiH]_0$ ratios of 50, 75, 100, 150, and 200. Table 1 lists the polymerization results. All the SEC traces of the obtained polymers showed a unimodal distribution and shifted to the higher molecular mass region with increasing $[EOEAm]_0/[Me_2EtSiH]_0$ ratios, as shown in Fig. 1. The $M_{n,MALS}$ values of 10.5, 15.9, 21.8, 31.8, and 42.5 kg mol^{-1} agreed with the $M_{n,calcd}$ values of 10.8, 16.1, 21.5, 32.3, and 43.0 kg mol^{-1}, respectively. The $Đ$s of the obtained polymers decreased from 1.15 to 1.10 with increasing $[EOEAm]_0/[Me_2EtSiH]_0$ ratios. These results indicated that $PEOEAm_x$ with the targeted DPs, *i.e.*, $PEOEAm_{50}$, $PEOEAm_{75}$, $PEOEAm_{100}$, $PEOEAm_{150}$ and $PEOEAm_{200}$, can be prepared by the hydrosilylation-promoted GTP of EOEAm by varying the $[EOEAm]_0/[Me_2EtSiH]_0$ ratios (Table 1).

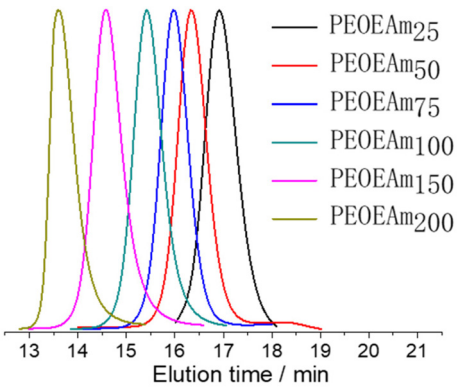

Fig. 1 Size-exclusion chromatography (SEC) traces of PEOEAm obtained by the GTP of EOEAm and Me_2EtSiH with $[EOEAm]_0/[Me_2EtSiH]_0$ ratios of 25, 50, 75, 100, 150, and 200 and with a $[Me_2EtSiH]_0/[B(C_6F_5)_3]_0$ ratio of 0.5.

Polymerization reactivity of EOEAm

The GTP method allows the synthesis of a variety of thermoresponsive PEOEAm-based polymers by using EOEAm for synthesizing copolymers and homopolymers. Therefore, we investigated the polymerization reactivity of EOEAm as well as the copolymerization of EOEAm and *N*,*N*-dimethylacrylamide (DMAm), the simplest *N*,*N*-disubstituted acrylamide. The resulting poly(*N*,*N*-dimethylacrylamide) (PDMAm) was water soluble but non-thermally expandable, similar to the reference monomer. First, the difference between the polymerization properties of EOEAm and DMAm was investigated through

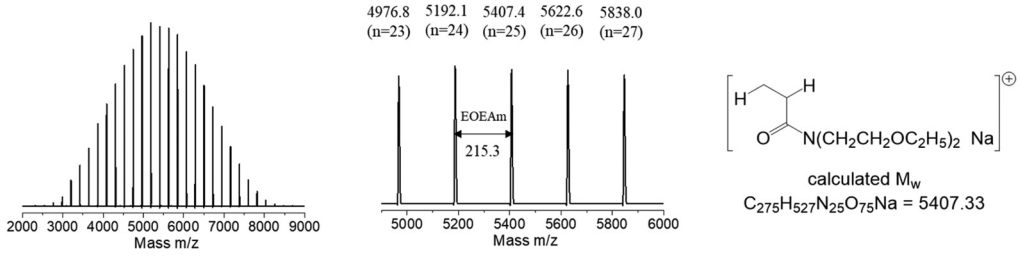

Fig. 2 Matrix assisted laser desorption/ionization-time of flight mass spectrometry (MALDI-TOF MS) spectra of representative PEOEAm with an $M_{n,MALS}$ of 5.4 kg mol^{-1} and an M_w/M_n of 1.20 (Table 1, run 1).

kinetic experiments using the hydrosilylation-promoted GTP under the following conditions: [EOEAm or DMAm]$_0$/[Et_2MeSiH]$_0$/[$B(C_6F_5)_3$]$_0$ = 100/1/0.1 and [EOEAm or DMAm]$_0$ = 1.0 mol L^{-1}. In both GTPs, induction periods were observed as shown in Fig. 3a, and induction times were 30 and 20 min for EOEAm and DMAm, respectively. After the induction time, both monomers were linearly consumed with different polymerization times, and the observed propagation rates ($k_{p.obs}$s) for EOEAm and DMAm were 8.8 and 68.2 min^{-1}, respectively, from the zero-order kinetic plots for monomer conversion (Conv.) *vs.* polymerization time (Time). The molecular mass (M_n) of the obtained polymers increased linearly with increasing monomer conversion, while the dispersity values ($Đ$s) remained below 1.2, as shown in Fig. 3b. These results indicate that the hydrosilylation-promoted GTP of EOEAm with Me_2EtSiH using $B(C_6F_5)_3$ proceeded in a controlled/living manner similar to the case of DMAm, while the polymerization rate of EOEAm was much slower than that of DMAm.[43–45]

Furthermore, to clarify the copolymerization reactivity of EOEAm toward DMAm, random group transfer copolymerization (GTcoP) of EOEAm and DMAm was performed under the conditions [EOEAm + DMAm]$_0$/[SKA^{Et}]$_0$/[$B(C_6F_5)_3$]$_0$ = 100/1/0.2 in CH_2Cl_2 (see the ESI†). The monomer reactivity ratios r_{EOEAm} and r_{DMAm} were determined to be 0.66 and 15.83, respectively, by the Kelen–Tüdös method. The reactivity of vinyl monomers is mainly affected by the electronegativity of the vinyl group and the steric hindrance around the vinyl group, and it is known that there exists a correlation between the electronegativity of the vinyl group and the chemical shift value in the ^{13}C NMR spectrum. The chemical shifts of CH_2= and –CH= for EOEAm are 128.14 and 127.57 ppm, respectively, which are very close to the values of 127.69 and 127.41 ppm for DMAm. Since the electronegativity of both monomers is almost equal, the factor that drastically reduced the polymerization properties of EOEAm compared to those of DMAm was mainly the bulky bis(2-ethoxyethyl)amino group in EOEAm.[46]

Block and random GTcoP

To expand the scope of thermoresponsive PEOEAm, block and statistical copolymers consisting of PEOEAm and PDMAm were prepared. The block GTcoP of EOEAm and DMAm was performed using the sequential addition of a monomer with different initial monomer feed ratios of [EOEAm]$_0$ and [DMAm]$_0$. The quantitative consumption of EOEAm in the first GTP was confirmed by ^1H NMR; thereafter, a second GTP was initiated by adding DMAm. In addition, the progress of the block GTcoP was confirmed by the shifting of the SEC trace of the polymer obtained from the first GTP of EOEAm to the high molecular mass region by the second GTP of DMAm while maintaining narrow molecular mass dispersions (Fig. S7†). In the case of the GTcoP with a [EOEAm]$_0$/[DMAm]$_0$/[Me_2EtSiH]$_0$/[$B(C_6F_5)_3$]$_0$ ratio of 50/50/1/1, the M_n ($Đ$) of the obtained polymer increased from 10.7 kg mol^{-1} (1.12) for the first GTP to 15.4 kg mol^{-1} (1.10) for the second GTP; this value agrees with $M_{n,cald}$ = 15.7 kg mol^{-1} (run 9, Table 2 and Fig. S7c†).

The random GTcoP of PEOEAm and PDMAm was expected to produce a gradient copolymer, not a random copolymer because there was an extremely large difference in the monomer reactivity ratio between the r_{EOEAm} of 0.66 and the r_{DMAm} of 15.83. This expectation was supported by the number-average sequence length of EOEAm units (l_{EOEAm}), which could be determined as a parameter reflecting the tendency to isolate the EOEAm–EOEAm diad. For the mole fractions of EOEAm of 0.3 and 0.8 in the monomer feed, l_{EOEAm} was very short, 1.1 and 3.6, respectively (Table S1†).[47–49] The random GTcoP of EOEAm and DMAm with the [Me_2EtSiH]$_0$/[$B(C_6F_5)_3$]$_0$ ratio of 1/0.2 should produce gradient copolymers (Table S1†), but the formation of block copolymers was achieved by the random GTcoP by increasing the amount of catalyst [Me_2EtSiH]$_0$/[$B(C_6F_5)_3$]$_0$ from 1/0.2 to 1/0.5. The polymerization progress for the random GTcoP of EOEAm and DMAm with the [EOEAm + DMAm]$_0$/[Me_2EtSiH]$_0$/[$B(C_6F_5)_3$]$_0$ ratio of (50 + 50)/1/0.5 in CD_2Cl_2 was followed by measuring the ^1H NMR spectra at polymerization times of 20, 40, and

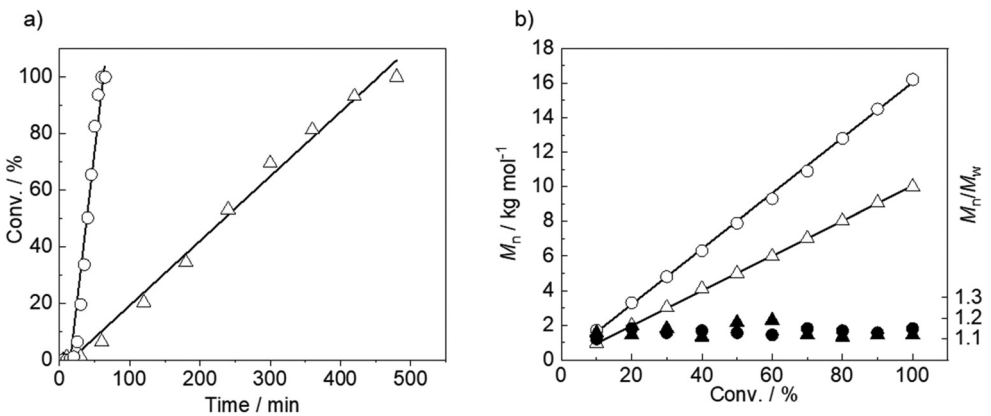

Fig. 3 (a) Zero-order kinetic plots and (b) dependence of molar mass (M_n) and molar mass distribution (M_w/M_n) on monomer conversion (Conv.) in the GTP of (○) EOEAm and (△) DMAm ([EOEAm or DMAm]$_0$/[Me_2EtSiH]$_0$/[$B(C_6F_5)_3$]$_0$, 100/1/0.1; [EOEAm or DMAm]$_0$, 1.0 mol L^{-1}).

590 min (Fig. 4). The characteristic proton absorptions attributed to the ═CH–CON– (6.56–6.62 ppm) and CH_3N– (3.02–3.09 ppm) groups of DMAm decreased at 20 min and disappeared at 40 min, while those attributed to the –$NCH_2CH_2OCH_2$– (3.44–3.67 ppm) and ═CH–CON– (6.65–6.71 ppm) groups remained unchanged until 40 min; thereafter, the characteristic proton absorptions attributed to the –$NCH_2CH_2OCH_2$– and ═CH–CON– groups decreased and finally disappeared completely at 590 min. The ^{1}H NMR spectrum of the polymer that partially disappeared from the polymerization system after 40 min revealed the characteristic proton absorption attributed to the methylene (1.35–2.07 ppm) and methine (2.26–2.78 ppm) groups in the main chain and CH_3N– groups, confirming the formation of PDMAm (Fig. S2a†). Furthermore, the ^{1}H NMR spectrum of the polymer obtained after 590 min revealed the characteristic proton absorption attributed to the methyl group of the CH_3CH_2O– group and the methylene groups in the –$NCH_2CH_2OCH_2$– moiety along with the absorption signals of PDMAm, confirming the formation of PDMAm-*b*-PEOEAm (Fig. S2b†). These results indicate that the first GTP of DMAm proceeded preferentially to afford living PDMAm, which functioned as a macroinitiator to continue the second GTP of EOEAm, resulting in the formation of PDMAm-*b*-PEOEAm in the random GTcoP of EOEAm and DMAm. This means the one-pot synthesis of a diblock copolymer by a random copolymerization. Increasing the amount of catalyst $[Me_2EtSiH]_0/[B(C_6F_5)_3]_0$ from 1/0.2 to 1/0.5 further increased the difference between the rates of polymerization of DMAm and EOEAm. The random GTcoP of EOEAm and DMAm was performed by varying the initial molar ratio of EOEAm and DMAm under the conditions $[EOEAm + DMAm]_0/[Me_2EtSiH]_0/[B(C_6F_5)_3]_0$ = 100/1/0.5. The copolymerization results of runs 14–20 are summarized in Table 2. For the obtained copolymer $PDMAm_y$-*b*-$PEOEAm_x$, the $M_{n,SEC}$ values were 13.4 kg mol^{-1} for *x*/*y* = 30/70, 14.4 for 40/60, 15.8 for 50/50, 16.7 for 60/40, 18.4 for 70/30, 19.6 for 80/20, and 20.1 for 90/10, which were in good agreement with the $M_{n,calcd}$ values. The *Đ* values were as small as 1.09–1.12.

The one-pot method was employed to synthesize tri- and tetra-block copolymers. After the first GTcoP of EOEAm and DMAm leading to PDMAm-*b*-PEOEAm, DMAm was sequentially added to the first living GTcoP system to afford PDMAm-*b*-PEOEAm-*b*-PDMAm. For extending the system from di- to tri-block segments, the unimodal SEC trace of the diblock copolymer shifted to a higher molar mass region after the second GTP, and the *Đ* was as low as 1.09–1.12 (Fig. S9†). The $M_{n,SEC}$ values of the obtained copolymers were 13.5, 14.6, 15.8, 17.1, 17.9, 19.3, and 20.5 kg mol^{-1}, which agreed well with the $M_{n,calcd}$ values of 13.4, 14.6, 15.7, 16.9, 18.0, 19.2, and 20.4 kg mol^{-1}, respectively (Table 3). The characteristic absorptions attributed to PDMAm and PEOEAm were observed in the ^{1}H NMR spectra of the obtained polymers, confirming the formation of $PDMAm_{25}$-*b*-$PEOEAm_{50}$-*b*-$PDMAm_{25}$ (Fig. S4†). Similarly, the first GTP of EOEAm, followed by the second GTcoP of PEOEAm and PDMAm, led to the synthesis of PEOEAm-*b*-PDMAm-*b*-PEOEAm. The extension process from di- to tri-block segments was confirmed from the SEC traces (Fig. S10†). The $M_{n,SEC}$ of the obtained copolymer agreed with the $M_{n,calcd}$ (runs 28–34, Table 3), and the *Đ* values were as low as 1.10–1.13. The formation of $PEOEAm_{25}$-*b*-$PDMAm_{50}$-*b*-$PEOEAm_{25}$ was confirmed from the ^{1}H NMR spectrum of the resulting copolymer (Fig. S5†). Finally, a tetra-block copolymer $(PDMAm\text{-}b\text{-}PEOEAm)_2$ was easily synthesized by repeating the random GTcoP of PEOEAm and PDMAm twice (Scheme 2).

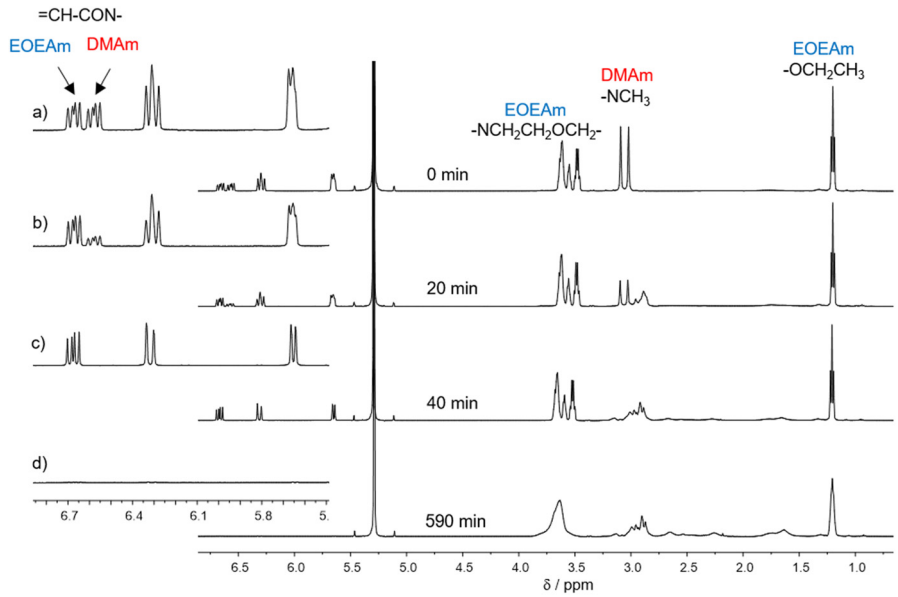

Fig. 4 ^{1}H nuclear magnetic resonance (NMR) spectra for the GTcoP of EOEAm and DMAm at polymerization times of (a) 0, (b) 20, (c) 40, and (d) 590 min and the expanded spectra of the vinyl groups of EOEAm and DMAm (solvent, CD_2Cl_2; $[EOEAm + DMAm]_0/[Me_2EtSiH]_0/[B(C_6F_5)_3]_0$, (50 + 50)/1/0.5; $[EOEAm + DMAm]_0$, 1.0 mol L^{-1}).

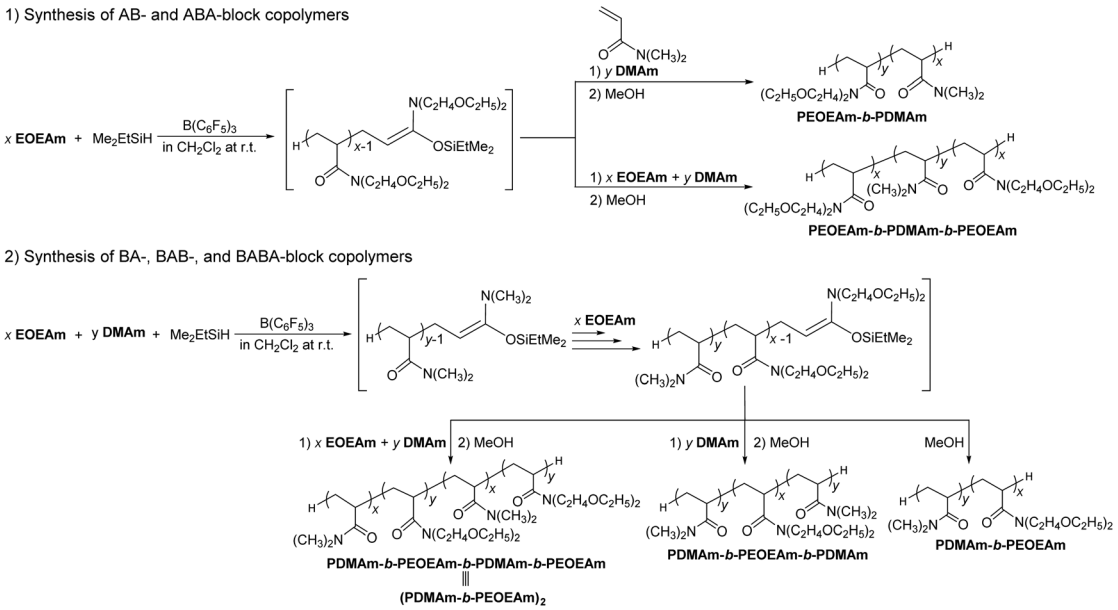

Scheme 2 Synthesis of (1) PEOEAm-*b*-PDMAm and PEOEAm-*b*-PDMAm-*b*-PEOEAm and (2) PDMAm-*b*-PEOEAm, PDMAm-*b*-PEOEAm-*b*-PDMAm, and (PDMAm-*b*-PEOEAm)$_2$ by the block and random GTcoP of EOEAm and DMAm.

SEC traces revealed that the extension from di- to tetra-block segments proceeded with $Đ$ values being maintained low (Fig. S11†), and the $M_{n,SEC}$ of the obtained copolymer agreed with the $M_{n,calcd}$ (Table 4). The formation of (PDMAm$_{25}$-*b*-PEOEAm$_{25}$)$_2$ was confirmed from the ^{1}H NMR spectrum of the resulting copolymer (Fig. S6†).

Thermoresponsive properties of PEOEAm and its copolymers with PDMAm

The thermal phase transition behaviors of PEOEAm and its copolymers were evaluated at the cloud-point temperature (T_{cp}). At T_{cp}, the transmittance reached 50% of the transmittance–temperature curve that was plotted by monitoring a polymer solution at a concentration of 10 g L^{-1} with a UV–vis spectrophotometer at a wavelength of 500 nm. The phase-transition properties of PEOEAm were compared with those of its analog, namely, poly(*N*,*N*-bis(2-methoxyethyl)acrylamide) (PMOEAm), to investigate the effect of the side chain of the monomer unit on the thermoresponsive properties. Fig. 5a shows the dependence of T_{cp} on the degree of polymerization (DP$_x$) of PEOEAm and PMOEAm. For both polymers, with increasing DP$_x$, T_{cp} decreased from 14.5 to 5.0 °C for PEOEAm and from 56.5 to 48.0 °C for PMOEAm. The T_{cp} of PEOEAm was drastically reduced because of the increase in hydrophobicity caused by the change in the side chain moiety of the ROCH$_2$CH$_2$N– group from methyl to ethyl groups. Such a decrease in T_{cp} (associated with the change from methyl to ethyl groups at the end of the ethylene oxide side chain) was observed for poly(glycidyl ether) and polyisocyanate with ethylene oxide (EO) side chains. Molecular-dynamics (MD) simulations for poly(glycidyl ether) with EO side chains indicated that the hydrophobic hydration shell around the ethyl group at the end of the side chain had a lower hydration shell density than that around the methyl group at the end of the side chain and was more easily broken upon increasing the temperature.[50–52] The MD simulations also showed that the fluctuations in the polymer chain for the ethyl group at the end of the side chain were smaller than those for the methyl

Table 4 Thermoresponsive properties of (PDMAm-*b*-PEOEAm)$_2$ by one-pot synthesis using the hydrosilylation-promoted GTcoP of EOEAm and DMAm with Me$_2$EtSiH using B(C$_6$F$_5$)$_3$ as the catalyst[a]

Run	Polymer	[EOEAm/DMAm]$_0$	Time/h	$M_{n,calcd}$/kg mol^{-1}	$M_{n,SEC}$ (M_w/M_n)[b]/kg mol^{-1}	T_{cp}[c]/°C
35	(PDMAm$_{35}$-*b*-PEOEAm$_{15}$)$_2$	15/35 × 2	8 + 12	13.4	13.9 (1.19)	57.8
36	(PDMAm$_{30}$-*b*-PEOEAm$_{20}$)$_2$	20/30 × 2	8 + 18	14.6	14.7 (1.20)	54.6
37	(PDMAm$_{25}$-*b*-PEOEAm$_{25}$)$_2$	25/25 × 2	8 + 18	15.7	15.8 (1.21)	44.9
38	(PDMAm$_{20}$-*b*-PEOEAm$_{30}$)$_2$	30/20 × 2	8 + 18	16.9	17.1 (1.21)	41.3
39	(PDMAm$_{15}$-*b*-PEOEAm$_{35}$)$_2$	35/15 × 2	12 + 24	18.0	18.2 (1.18)	38.1
40	(PDMAm$_{10}$-*b*-PEOEAm$_{40}$)$_2$	40/10 × 2	12 + 24	19.2	19.6 (1.20)	25.5

[a] Solvent, CH$_2$Cl$_2$; temp., 25 °C; Ar atmosphere; [M]$_0$, 1.0 mol L^{-1}; [MOEAm + EOEAm]$_0$/[Me$_2$EtSiH]$_0$/[B(C$_6$F$_5$)$_3$]$_0$, 50/1/1; monomer conversion determined by ^{1}H NMR spectra in CDCl$_3$, >99.9%. [b] Determined by an SEC instrument equipped with an RI detector in DMF containing lithium chloride (0.01 mol L^{-1}) using PMMA standards. [c] Determined by UV–vis measurements in water (10 g L^{-1}).

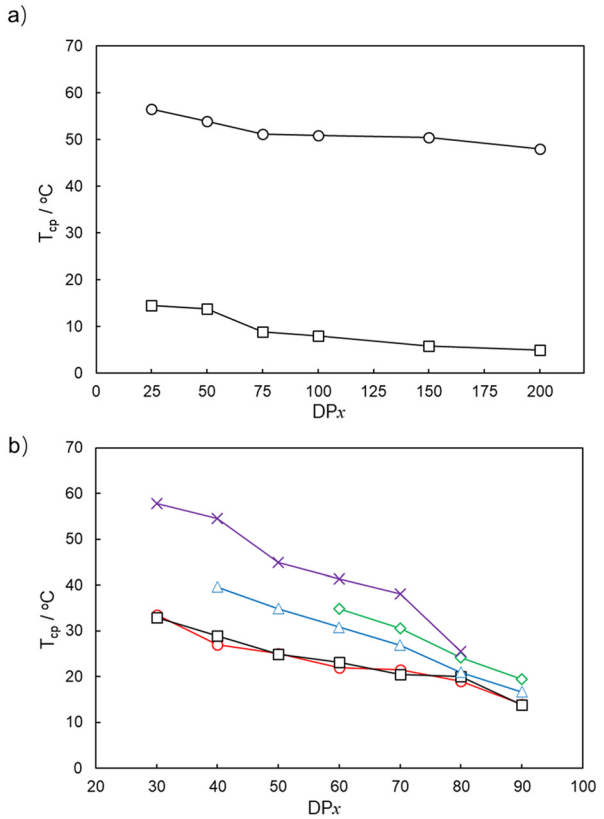

Fig. 5 Dependence of the cloud-point temperature (T_{cp}) on the degree of polymerization (DP_x) of (a) (□) $PEOEAm_x$ and (○) $PMOEAm_x$ and (b) (○) $PDMAm_y$-*b*-$PEOEAm_x$, (□) $PEOEAm_x$-*b*-$PDMAm_y$, (◊) $PDMAm_y$-*b*-$PEOEAm_x$-*b*-$PDMAm_y$, (Δ) $PEOEAm_x$-*b*-$PDMAm_y$-*b*-$PEOEAm_x$, and (x) $(PDMAm_{y/2}$-*b*-$PEOEAm_{x/2})_2$.

group at the end of the side chain, making it more difficult for water molecules to penetrate into the gaps between the side chains. This inhibiting effect of the ethyl group on the penetration of water into the gaps between the side chains, together with the hydrophobicity of the ethyl group itself, is thought to contribute to the lower T_{cp} of PEOEAm.

The thermoresponsive properties of the di-, tri-, and tetra-block copolymers are summarized in Fig. 5b. T_{cp} decreased with increasing DP_x of $PEOEAm_x$ for all the block copolymers and increased in the following order: PDMAm-*b*-PEOEAm ≈ PEOEAm-*b*-PDMAm < PEOEAm-*b*-PDMAm-*b*-PEOEAm < PDMAm-*b*-PEOEAm-*b*-PDMAm < $(PDMAm$-*b*-$PEOEAm)_2$. In the diblock copolymer system, the dependence of T_{cp} on DP_x was almost the same for both PDMAm-*b*-PEOEAm (14.0–33.6 °C) and PEOEAm-*b*-PDMAm (13.8–33.0 °C); this result supports the aforementioned conclusion that the copolymer obtained from the random GTcoP of EOEAm and DMAm is not a random structure but a block structure, *i.e.*, PDMAm-*b*-PEOEAm. In the triblock copolymer system, the T_{cp} values for PEOEAm-*b*-PDMAm-*b*-PEOEAm were about 3.5 °C higher than those for PDMAm-*b*-PEOEAm-*b*-PDMAm. No T_{cp} was observed for $PEOEAm_{15}$-*b*-$PDMAm_{70}$-*b*-$PEOEAm_{15}$ because it was insoluble in water; this result was different from that obtained for $PEOEAm_{30}$-*b*-$PDMAm_{70}$, which has a T_{cp} of 33.0 °C. Furthermore, $PDMAm_y$-*b*-$PEOEAm_x$-*b*-$PDMAm_y$ ($x + 2y = 100$) exhibited no thermoresponsive behavior for $x < 50$; this is unlike the case of $PEOEAm_x$-*b*-$PDMAm_y$ ($x + y = 100$), which exhibited thermal phase transition for x in the range of 30–90. These results indicated that the sequence of the two block segments in the triblock copolymer system greatly affected the thermoresponsive properties. For the tetra-block copolymer system, the thermoresponsive properties of $(PDMAm$-*b*-$PEOEAm)_2$ can be widely varied (T_{cp} varies from 25.5 to 57.8 °C), which is in contrast to the results obtained for PDMAm-*b*-PEOEAm, which has a narrow range of T_{cp} (14.0–33.6 °C). The thermoresponsive properties of PEOEAm can be controlled by forming its block copolymers with water soluble, non-thermoresponsive PDMAm, and the T_{cp} increases with an increasing number of blocks in the block copolymer in the following order: $PEOEAm_{50}$ (13.9 °C) < $PDMAm_{50}$-*b*-$PEOEAm_{50}$ (25.1 °C) < $PEOEAm_{25}$-*b*-$PDMAm_{50}$-*b*-$PEOEAm_{25}$ (34.9 °C) < $(PDMAm_{25}$-*b*-$PEOEAm_{25})_2$ (44.9 °C).

Finally, the thermal phase transition was further discussed using the hydrodynamic radii (R_hs) of block copolymers. Fig. S13† shows the distribution of R_h for $PDMAm_{50}$-*b*-$PEOEAm_{50}$, $PEOEAm_{50}$-*b*-$PDMAm_{50}$, $PDMAm_{25}$-*b*-$PEOEAm_{50}$-*b*-$PDMAm_{25}$, $PEOEAm_{25}$-*b*-$PDMAm_{50}$-*b*-$PEOEAm_{25}$, and $(PEOEAm_{25}$-*b*-$PDMAm_{25})_2$. Table 5 summarizes the R_h values measured at 20 and 50 °C. For the diblock copolymer system, the R_h values after the phase transition were about 40 times those before the phase transition; R_h values changed from 11.6 to 428.8 nm for $PDMAm_{50}$-*b*-$PEOEAm_{50}$ and from 11.4 to 411.5 nm for $PEOEAm_{50}$-*b*-$PDMAm_{50}$. There was little difference between the two diblock copolymers because the copolymer obtained by the random GTcoP was the diblock copolymer, PDMAm-*b*-PEOEAm. For the triblock copolymer system, the R_h values increased after the phase transition; they increased from 11.1 to 510.5 nm for $PEOEAm_{25}$-*b*-$PDMAm_{50}$-*b*-$PEOEAm_{25}$, whose sizes were similar to those of the diblock copolymers. In contrast, the R_h values of $PDMAm_{25}$-*b*-$PEOEAm_{50}$-*b*-$PDMAm_{25}$, which is not thermoresponsive, increased only approximately four times from 12.3 (before the phase transition) to 47.0 nm (after the phase transition). In addition, the R_h value increased from 13.7 (before the phase transition) to 572.9 nm (after the phase transition) for $(PEOEAm_{25}$-*b*-$PDMAm_{25})_2$; this result is similar to that obtained for the di- and triblock copolymer systems, except that $PDMAm_{25}$-*b*-$PEOEAm_{50}$-*b*-$PDMAm_{25}$ was insoluble in water. These results indicated that the di-, tri-, and tetra-block copolymers formed large, disordered aggregates in response to thermal stimuli, resulting in the aqueous copolymer solution changing from a clear to a turbid solution. Moreover, $PDMAm_y$-*b*-$PEOEAm_x$-*b*-$PDMAm_y$ with x = 30, 40, and 50 and $PEOEAm_{15}$-*b*-$PDMAm_{70}$-*b*-$PEOEAm_{15}$ could not measure thermal phase transitions because the aqueous solutions of these triblock copolymers were cloudy. The hydrophobicity of these triblock copolymers was unexpected because PEOEAm and PDMAm are soluble in water, but we confirmed that the arrangement of PEOEAm and PDMAm in the multiblock co-

Table 5 Hydrodynamic radii (R_hs) of $PDMAm_{50}$-*b*-$PEOEAm_{50}$, $PEOEAm_{50}$-*b*-$PDMAm_{50}$, $PDMAm_{25}$-*b*-$PEOEAm_{50}$-*b*-$PDMAm_{25}$, $PEOEAm_{25}$-*b*-$PDMAm_{50}$-*b*-$PEOEAm_{25}$, and $(PEOEAm_{25}$-*b*-$PDMAm_{25})_2$ at 20 and 50 °C

Polymer	T_{cp}[a]	R_h[b]/nm	
		20 °C	50 °C
$PDMAm_{50}$-*b*-$PEOEAm_{50}$	25.1	11.6	428.8
$PEOEAm_{50}$-*b*-$PDMAm_{50}$	25.0	11.4	411.5
$PDMAm_{25}$-*b*-$PEOEAm_{50}$-*b*-$PDMAm_{25}$	—	12.3	47.0
$PEOEAm_{25}$-*b*-$PDMAm_{50}$-*b*-$PEOEAm_{25}$	39.6	11.1	510.5
$(PDMAm_{25}$-*b*-$PEOEAm_{25})_2$	44.9	13.7	572.9

[a] Determined by UV–vis measurements in water (10 g L^{-1}). [b] Determined by dynamic light scattering (DLS) measurements in water (3 g L^{-1}).

polymer has a significant effect on the thermoresponsive properties. Therefore, further studies on the aggregation structure of the multiblock copolymers are needed by measuring the critical micelle concentration (CMC) and by molecular dynamics (MD) simulations.

Conclusions

The hydrosilylation-promoted GTP of EOEAm with Me_2EtSiH using the $B(C_6F_5)_3$ catalyst can precisely synthesize PEOEAm, with repeating units of EOEAm only and without initiator residues at the α chain end. The polymerization kinetics of the GTP of EOEAm or DMAm showed that the polymerization rate of EOEAm was much lower than that of DMAm. In the random GTcoP of EOEAm and DMAm, after all DMAm was consumed, the polymerization of EOEAm proceeded to produce not a statistical copolymer but a block copolymer, *i.e.*, the one-pot synthesis of PDMAm-*b*-PEOEAm. This method was used to synthesize tri- and tetra-block copolymers. The block copolymer of PEOEAm and PDMAm exhibited a thermal phase transition in which large, disordered aggregates formed in response to thermal stimuli, resulting in the aqueous copolymer solution changing from a clear to a cloudy solution. The T_{cp} values of 14.5–5.0 °C for PEOEAm were 40 °C lower than those of 56.5–48.0 °C for PMOEAm. Furthermore, the T_{cp} increased as the number of blocks in the block copolymer increased in the following order: PDMAm-*b*-PEOEAm ≈ PEOEAm-*b*-PDMAm < PEOEAm-*b*-PDMAm-*b*-PEOEAm < PDMAm-*b*-PEOEAm-*b*-PDMAm < $(PDMAm$-*b*-$PEOEAm)_2$. The exceptions were $PEOEAm_{15}$-*b*-$PDMAm_{70}$-*b*-$PEOEAm_{15}$ and $PDMAm_y$-*b*-$PEOEAm_x$-*b*-$PDMAm_y$ (x = 30, 40, and 50) that did not undergo any phase transition, possibly because these triblock copolymers formed stable micelles consisting of a hydrophobic PEOEAm core and a hydrophilic PDMAm shell; however, further clarification of this matter is needed. Even for a low-thermoresponsive polymer, by using its block copolymer with a water-soluble polymer, the thermoresponsive temperature could be controlled over a wide range by adjusting the DP ratio of two blocks and the number of blocks in the copolymer.

Conflicts of interest

The authors declare no conflict of interest.

Acknowledgements

This research was funded by the Recruitment Program of Global Experts, China, the Science and Technology Research Project of the Education Department of Jilin Province, grant number JJKH20210806KJ, the Youth Fund of Changchun University of Science and Technology, grant number YDZJ202301ZYTS298, and the Grant-in-Aid for Challenging Exploratory Research (22K19929029) from JSPS, Japan.

References

1 J. F. Mano, *Macromol. Biosci.*, 2010, **9**(6), 622–622.
2 J. S. Leng, X. Lan, Y. J. Liu, S. Y. Du, W. M. Huang, N. Liu, S. J. Phee and Q. Yuan, *Appl. Phys. Lett.*, 2008, **92**(1), 014104.
3 T. He, Y. Wang, A. Narumi, L. Xu, S. I. Sato, X. Shen and T. Kakuchi, *Polymers*, 2021, **13**(22), 3873.
4 J. Leng, X. Lan, Y. Liu and S. Du, *Prog. Mater. Sci.*, 2011, **56**(7), 1077–1135.
5 K. L. Deng, H. Tian and P. F. Zhang, *eXPRESS Polym. Lett.*, 2009, **3**(2), 97–104.
6 I. Chikh Alard, J. Soubhye, G. Berger, M. Gelbcke, S. Spassov, K. Amighi, J. Goole and F. Meyer, *Polym. Chem.*, 2017, **8**(16), 2450–2456.
7 M. Rajagopalan, J. H. Jeon and I. K. Oh, *Sens. Actuators, B*, 2010, **151**(1), 198–204.
8 J. Mao, X. Ji and S. Bo, *Macromol. Chem. Phys.*, 2011, **212**(7), 744–752.
9 J. Li, S. Mizutani, S. Sato, A. Narumi, O. Haba, S. Kawaguchi, M. Kikuchi, T. Kakuchi and X. Shen, *Polymer*, 2020, **202**, 122678.
10 R. Freitag, T. Baltes and M. Eggert, *J. Polym. Sci., Polym. Chem.*, 1994, **32**(16), 3019–3030.
11 A. Narumi, S. I. Sato, X. Shen and T. Kakuchi, *Polym. Chem.*, 2022, **13**, 1293–1319.
12 P. J. Roth, T. P. Davis and A. B. Lowe, *Macromolecules*, 2012, **45**(7), 3221–3230.
13 N. Zhang, S. Salzinger and B. Rieger, *Macromolecules*, 2012, **45**(24), 9751–9758.
14 J. Heyda, S. Soll, J. Yuan and J. Dzubiella, *Macromolecules*, 2014, **47**(6), 2096–2102.
15 A. L. Brocas, M. Gervais, S. Carlotti and S. Pispas, *Polym. Chem.*, 2012, **3**(8), 2148.
16 H. Y. Lee, S. H. Park, J. H. Kim and M. S. Kim, *Polym. Chem.*, 2017, **8**(43), 6606–6616.
17 S. J. T. Rezaei, M. R. Nabid, H. Niknejad and A. A. Entezami, *Int. J. Pharm.*, 2012, **437**(1–2), 70–79.
18 S. Ashraf, H. K. Park, H. Park and S. H. Lee, *Macromol. Res.*, 2016, **24**(4), 297–304.

19 D. Rusu, D. Ciolacu and B. C. Simionescu, *Cellul. Chem. Technol.*, 2019, **53**(9–10), 907–923.
20 R. S. Dhanikula and P. Hildgen, *Bioconjugate Chem.*, 2006, **17**(1), 29–41.
21 X. Wang and M. G. Mccord, *J. Appl. Polym. Sci.*, 2007, **104**(6), 3614–3621.
22 S. K. Filippov, A. Y. Bogomolova, L. Kaberov, N. Velychkivska, L. Starovoytova, Z. Cernochova, S. E. Rogers, W. M. Lau, V. V. Khutoryanskiy and M. T. Cook, *Langmuir*, 2016, **32**(21), 5314–5323.
23 A. Papagiannopoulos, J. Zhao, G. Zhang, S. Pispas and A. Radulescu, *Eur. Polym. J.*, 2014, **56**, 59–68.
24 S. M. Benjamin, R. R. Jorge, L. Marco, F. B. Antonio and L. C. Enrique, *Adv. Colloid Interface Sci.*, 2014, **205**(1), 113–123.
25 M. Panayiotou, C. Poehner, C. Vandevyver, C. Wandrey, F. Hilbrig and R. Freitag, *React. Funct. Polym.*, 2007, **67**(9), 807–819.
26 M. Kobayashi, S. Okuyama, T. Ishizone and S. Nakahama, *Macromolecules*, 1999, **32**(20), 6466–6477.
27 C. W. Kan, E. A. S. Doherty and A. E. Barron, *Electrophoresis*, 2003, **24**(24), 4161–4169.
28 C. C. Rafael, L. Schellkopf, F. L. Cristina, P. S. Isabel and P. J. Jorge, *Langmuir*, 2015, **31**(3), 1142–1149.
29 J. Kido, Y. Imamura, N. Kuramoto and K. Nagai, *J. Colloid Interface Sci.*, 1992, **150**(2), 338–343.
30 M. Horecha, V. Senkovskyy, M. Stamm and A. Kiriy, *Macromolecules*, 2009, **42**(15), 5811–5817.
31 S. Kikuchi, Y. Chen, E. Ichinohe, K. Kitano, S. Sato, Q. Duan, X. Shen and T. Kakuchi, *Macromolecules*, 2016, **49**(13), 4828–4838.
32 M. Hechenbichler, A. Laschewsky and M. Gradzielski, *Colloid Polym. Sci.*, 2021, **299**(2), 205–219.
33 A. H. Hofman, G. O. R. Alberda van Ekenstein, A. J. J. Woortman, G. Brinke and K. Loos, *Polym. Chem.*, 2015, **6**(39), 7015–7026.
34 T. Hidaka, S. Sugihara and Y. Maeda, *Eur. Polym. J.*, 2013, **49**(3), 675–681.
35 D. Babuka, K. Kolouchova, M. Hruby, O. Groborz, Z. Tosner, A. Zhigunov and P. Stepanek, *Eur. Polym. J.*, 2019, 109306.
36 Z. Song, K. Wang, C. Gao, S. Wang and W. Zhang, *Macromolecules*, 2015, **49**(1), 162–171.
37 G. Delaittre, J. Rieger and B. Charleux, *Macromolecules*, 2011, **44**(3), 462–470.
38 B. Yamada, M. Yoshioka and T. Otsu, *J. Polym. Sci., Polym. Chem.*, 1984, **22**(2), 463–473.
39 J. Li, S. Kikuchi, S. Sato, Y. Chen, L. Xu, B. Song, Q. Duan, Y. Wang, T. Kakuchi and X. Shen, *Macromolecules*, 2019, **52**(19), 7207–7217.
40 S. Kikuchi, Y. Chen, K. Kitano, K. Takada, T. Satoh and T. Kakuchi, *Polym. Chem.*, 2015, **6**(38), 6845–6856.
41 J. Li, S. Mizutani, S. Sato, A. Narumi, O. Haba, S. Kawaguchi, M. Kikuchi, T. Kakuchi and X. Shen, *Polym. Chem.*, 2020, **11**(13), 2346–2359.
42 S. Kikuchi, Y. Chen, K. Kitano, S. Sato, T. Satoh and T. Kakuchi, *Macromolecules*, 2016, **49**(8), 3049–3060.
43 P. L. Nayak, S. Lenka and P. K. Nayak, *J. Appl. Polym. Sci.*, 1992, **45**(4), 655–661.
44 F. Tüdos, T. Kelen, T. Földes-berezsnich and B. Turcsányi, *Polym. Bull.*, 1980, **2**(1), 71–76.
45 F. Tüdos, T. Kelen, T. Földes-berezsnich and B. Turcsányi, *J. Macromol. Sci., Part A: Pure Appl.Chem.*, 1976, **10**(8), 1513–1540.
46 N. Gatica, N. Fernández, A. Opazo, S. Alegría, L. Gargallo and D. Radic, *Polym. Int.*, 2003, **52**(8), 1280–1286.
47 L. Han, G. Zhu, W. Zhang and W. Chen, *J. Appl. Polym. Sci.*, 2009, **113**(2), 1298–1306.
48 S. Collins, A. M. Kenwright, C. Pawson, S. K. Peace, R. W. Richards, W. A. MacDonald and P. Mills, *Macromolecules*, 2000, **33**(8), 2974–2980.
49 Q. Niu, C. Zou, X. Liu, R. Wang and A. He, *Polymer*, 2017, **109**, 197–204.
50 E. Terada, T. Isono, T. Satoh, T. Yamamoto, T. Kakuchi and S. Sato, *Nanomaterials*, 2023, **13**(10), 1628.
51 K. Miyachi, S. Sato, T. Kakuchi, T. Isono, T. Satoh and Y. Satoh, *Polym. Chem.*, 2017, **8**, 5698–5707.
52 N. Sakai, M. Jin, S. I. Sato, T. Satoh and T. Kakuchi, *Polym. Chem.*, 2014, **5**, 1057–1062.

